

UDK 546.831, 666.3.019

Determination of Degradation Level during Cavitation Erosion of Zircon Based Ceramic

Marko Pavlović¹, Marina Dojčinović¹, Sanja Martinović^{2*)}, Milica Vlahović², Zoran Stević³, Marina Jovanović⁴, Tatjana Volkov-Husović¹

¹University of Belgrade, Faculty of Technology and Metallurgy, 4 Karnegijeva St., Belgrade, Serbia

²University of Belgrade, Institute of Chemistry, Technology and Metallurgy, 12 Njegoševa St., Belgrade, Serbia

³University of Belgrade, Technical Faculty in Bor, 12 Vojske Jugoslavije St., Bor, Serbia

⁴Faculty of Metallurgy and Materials Science, University of Zenica, Bosnia and Herzegovina

Abstract:

Mechanical shock of zircon based ceramic induced by cavitation erosion testing was investigated in this study. Several parameters were followed in order to determine level of material degradation during the cavitation erosion testing. Mass loss was taken as a conventional criterion for material degradation, while the level of surface degradation was evaluated by image and thermal imaging analyses. Results show high cavitation resistance of zircon ceramics and their suitability when vigorous cavitation erosion environment is expected.

Keywords: *zircon based ceramic; cavitation erosion; mass loss; image analysis; thermal imaging.*

1. Introduction

Zircon ($ZrSiO_4$) is an attractive refractory material, which is widely used for the synthesis of new materials due to its properties: high melting temperature or high refractoriness, low coefficient of thermal expansion, high resistance to thermal shock, not wetted with liquid metal, minimal gas production when in contact with liquid metal [1-4]. An important application of zircon based ceramics is found in the foundry for making molds for casting of high-quality steel castings, manufacturing ceramic shells, and ceramic cores in investment casting. Refractory coatings based on zircon are recommended for casting of high temperature materials [5]. Also, filler based on zircon with certain grain size and shape provides the best resistance to penetration of liquid metal in the mold and contributes to obtain a high quality surface of castings. This filler is used in the coating composition for casting large or complex steel castings, and where rapid heat dissipation from the materials is necessary [1, 4, 6, 7]. Due to good mechanical properties, zircon was investigated for the synthesis of various ceramic composites as well as their testing and application for different condition. It was assumed that zircon will show good resistance in extreme condition such as

*) Corresponding author: smartinovic@tmf.bg.ac.rs

subjecting to the cavitation erosion. Namely, cavitation erosion is a phenomenon usually observed in many types of hydraulic structures and engineering installations such as ship propellers, pumps, hydraulic turbines or valves, while the metallic materials is mostly used for the synthesis of the components that should be exposed to the cavitation. Recent studies are mainly occupied by replacement of metallic components with composite and ceramic materials as well as to enhance the erosion resistances of different alloys and steels by deposition of protective coatings on their surfaces [8-26]. Therefore, the reliable approach to analyze and predict the risk of cavitation erosion of different materials used in such conditions is very welcome. Synthesis and characterization of the zircon based ceramics with the aim of applying in the vigorous exploitation conditions of cavitation erosion was performed in this study. In order to monitor behaviour of zircon sample in such condition, conventional method of measuring the mass loss was applied. In addition, image and thermal imaging analyses are also implemented for better understanding of material degradation induced by the cavitation [8, 9, 24, 25, 27-36]. This approach is useful for the assessment of cavitation resistance of zircon based ceramics and possibilities of its future application in practice.

2. Experimental

2.1 Synthesis and Characterization

High purity zircon (99.99 wt.% $ZrSiO_4$) was used for the sample synthesis. Zircon was obtained by mechanical processing, purifying, and milling of refractory mineral raw materials—zircon sand. Zircon based powder was ground to the grain size of 25 μm in a vibratory mill. The samples for testing were obtained by pressing powder into tablets with a diameter of $2 \cdot 10^{-2}$ m, using the Leitz pressure device with applied pressure of 10^6 Pa. Afterwards, the zircon samples were sintered at temperature of 1200 °C. The sintering regime process was carried out according to the following mode: raising the temperature to 1000 °C with a heating rate of 5 °C/min in a time of 200 min; then, heating up to 1200 °C with heating rate of 2 °C/min in a time of 100 min; sintering at 1200 °C in a time of 1 hour.

X-ray diffraction analysis of sintered zircon sample was done by the X-ray diffractometer PHILIPS, model PW-1710.

Microstructure of the sintered zircon sample was characterized by scanning electron microscopy method (SEM) using a JOEL JSM-6390LV microscope.

2.2 Methods

2.2.1 Cavitation erosion testing

Cavitation erosion testing was performed using ultrasonic vibration method (with stationary specimen) according to standard procedure [14, 15]. The usual characteristics for the frequency and peak-to-peak displacement amplitude of the horn were used, as well as characteristics of liquid are described in details in previous papers [8, 9, 16, 24-25].

Based on the standard procedure, the specimen is weighed before and periodically during the test in order to obtain mass loss versus time or cumulative erosion versus time curve. Measuring the mass loss was performed after each exposure interval of 10 minutes for the test period of 80 min. Before the test and after each test interval, the specimens were dried at 110 °C for an hour. Mass loss was measured using analytical balance with an accuracy of ± 0.1 mg.

Besides conventional monitoring of material damage exposed to the cavitation which included measuring the mass loss, image and thermal imaging analyses were also applied with the aim to determine surface degradation level of the sample. For the further experiments related to monitoring of damage occurrence and its growth during the testing, samples were photographed using CCD and IR cameras before and during the cavitation erosion testing.

2.2.2 Image analysis

Monitoring of the surface erosion caused by the cavitation and hence the surface damage level were performed by image analysis as an addition to the standard laboratory procedure of the mass loss measuring [8, 9, 24-25]. Image Pro Plus (IPP) program [27] was used in analysis of the sample surfaces. Results were given as the surface degradation level (P/P_0) during the testing time. P_0 (level of degradation before the testing) was determined according to the ideal surface (surface area without any defects). P was measured as surface area that was destructed during the cavitation testing. Behavior of tested material exposed to the cavitation can be analyzed by correlating surface degradation level and material properties.

Besides the implementation of image analysis on determination of surface degradation level during the testing, it is also possible to use it for obtaining the line profile and measuring the diameter and area of the erosion ring region in order to estimate amount and size of existing pits. Applied measurements give us the possibility to study the complex changes that occurred in the sample during testing time not only with the aim to measure the erosion intensity by monitoring formation of new pits and growth of already existing pits but also to analyze behavior of tested material and predict its durability.

2.2.3 ThV testing

Two IR lamps of 250 W were used as thermal excitation source in the investigation. The IR camera FLIR E60 had the spectral range 7.5 - 13 μm , 50 mK at 30 °C thermal sensitivity, MSX 320 x 240 resolution, and frame rate of 60 Hz. FLIR Tools and software were used in determination of the temperature profiles and histograms in the post-processing of thermogram sequences after heating step.

3. Results and Discussion

3.1 Phase composition of zircon sample

Diffraction pattern of zircon sintered at temperature of 1200 °C (Fig. 1) shows clearly expressed picks characteristic for high purity zircon, so the dominant mineral phase in tested sample is zircon.

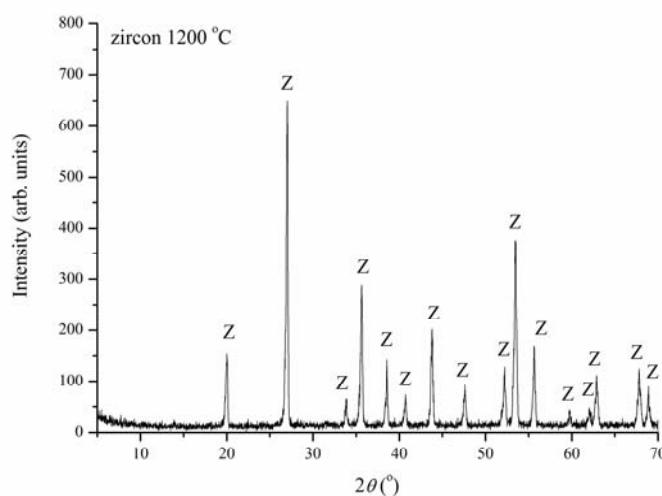


Fig. 1. XRD pattern of zircon sample sintered at 1200 °C (Z - ZrSiO₄).

3.2 Microstructural analysis of zircon sample

SEM analysis of zircon sample sintered at 1200 °C is given in Fig. 2. Microphotography shows uniform structure with high density and very little porosity (dark part of the surface).

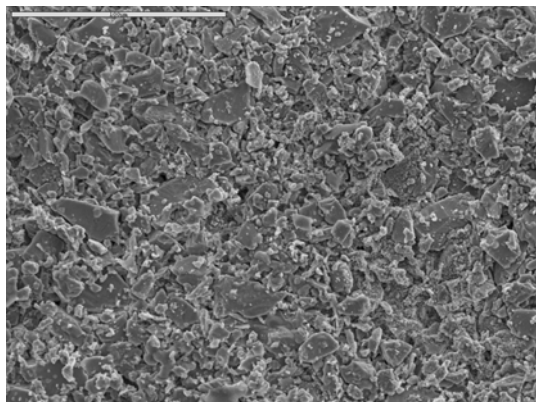


Fig. 2. SEM microphotographs of zircon sample sintered at 1200 °C.

3.3 Mass change

Monitoring mass changes of the samples during exposure to the cavitation included measuring the weight loss compared to initial weight before the testing. Total mass loss results of a sintered zircon sample as a function of exposure time are given in Fig. 3, showing typical cumulative mass loss curve.

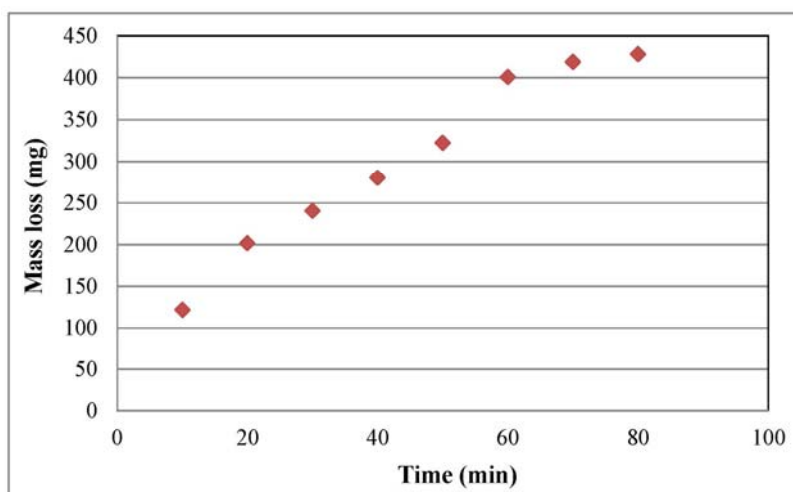


Fig. 3. Cumulative mass loss of zircon sample during the cavitation erosion testing.

By analyzing the erosion progression, it is evident that incubation period in the early stage of the damaging is very short since the period without loss of material is almost negligible according to the chosen experimental conditions (cavitation exposure period of 10 min). As the exposure time to the cavitation increases, cumulative mass loss of the sintered zircon sample gradually increases almost linearly till 60 minutes. During this period, which is also known as acceleration period, material suffers a significant deterioration and weight loss until attaining a maximum value. This erosion rate increase can be interpreted with structure and properties of zircon, tetragonal crystal structure, high mechanical properties, particularly large hardness. Besides, by grinding of zircon samples to the grain size of 25 μm , zircon

becomes mechanically activated. After 60 minutes of exposure to the cavitation, mass loss is slightly slowing down and reaching deceleration erosion period. Obtained results indicate good resistance of tested zircon sample.

3.4 Image analysis

Sintered zircon samples were photographed before and during the cavitation erosion testing, Fig. 4.

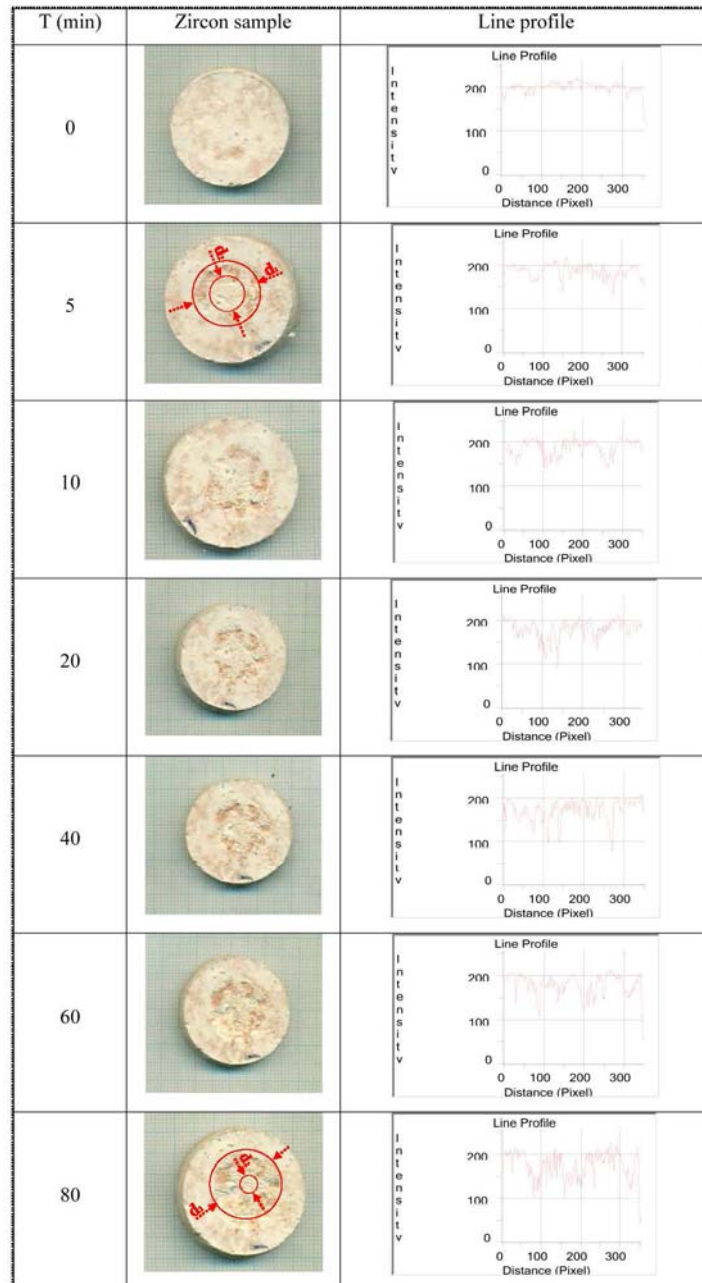


Fig. 4. Photographs and line profiles of the samples before and during cavitation erosion testing.

Figure 4 shows that degradation of the sample begins almost immediately, as the first pits are formed after only 5 minutes. Damage level during the testing was determined using

IPP program and the results are given in Fig. 5. Level of surface degradation is linearly increasing up for almost whole period of testing, except for the cavitation exposure interval between 70 and 80 minutes where the increase of surface degradation level occurred slower.

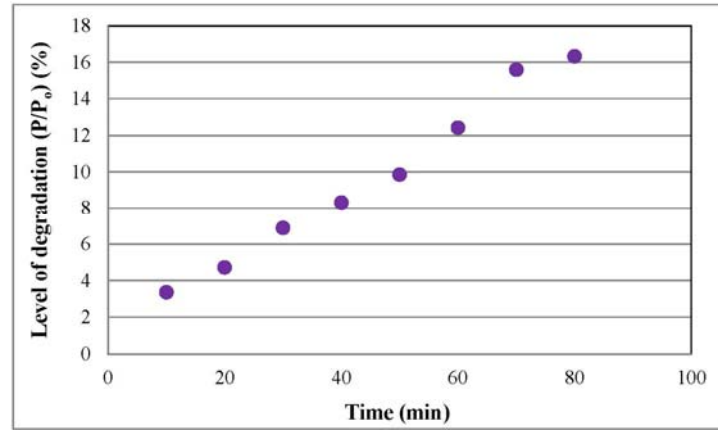


Fig. 5. Level of the surface degradation.

On the one hand the mass loss occurs rapidly up to 60 minutes and slows down thereafter, but on the other hand level of surface degradation develops rapidly up to 70 minutes while after that it goes slower. These two seemingly opposite facts can be explained by the formation of small tiny shallow pits with small mass loss occurring but they surely cause damages at the surface and increase the damaged area. Discussion occupied with analysis of ring diameter shown below can clarify this phenomenon.

A characteristic pit occurred after 80 minutes of cavitation erosion testing is given in Fig. 6. The pit with small depth indicates very good resistance of sintered zircon based sample.

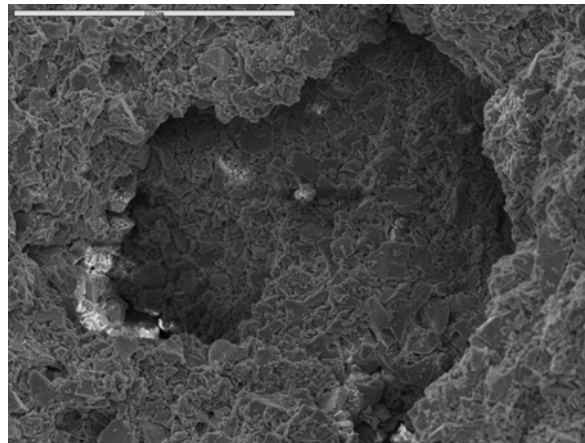


Fig. 6. SEM photograph of the zircon samples after cavitation erosion.

Image Pro Plus program allows access to lines of profiles that are used to analyze the level of sample surface degradation. In this process, the appropriate color channel was chosen and applied on the images of the sintered zircon samples and RGB mode was selected. Image samples were analyzed using red, blue, and green channels. The best resolution between damaged and undamaged surface was achieved using blue color channels. After choosing filter channel, line profile option by sample diameter was applied. Figure 4 shows photographs of sintered zircon samples during cavitation testing and the corresponding line profiles.

The development of surface degradation during the testing is clearly evident, while the line profiles obviously indicate increase of the degradation. Also, it is noticeable that the peaks are higher at the center of the sample where the pits are occurred. These findings correspond to the results of measuring the level of surface degradation. This approach in research and assessment of resistance of zircon samples to the effects on cavitation erosion can be useful in practice for the purpose of estimating the lifetime of the product based on zircon.

Some ceramic materials such as silicon carbide–cordierite ceramics [37] and commercially available silicon nitride and zirconia balls [38] form characteristic erosion ring. Besides mass loss and degraded surface area, it is possible to measure degradation level during the cavitation by determining the inner (d_2) and outer (d_1) ring diameters and monitoring the changes of these values during the testing. Also, the average areas of degraded surfaces can be calculated by using IPP program. It is obvious that the outer diameter corresponds to the diameter of the horn, while the inner diameter presents diameter of the area where small pits were observed. Measuring both ring diameters during the exposure to the cavitation was done by using the images in Figure 4 and applying the software for image analysis (IPP). Since the surface changes were noticed around the area of inner ring, obtained results related to the changes of inner ring diameter and area are shown in Figures 7 and 8. Unlike previously published papers [37, 38] where the ring diameter and surface area of small pits were increasing during the experiment, tested zircon sample behaved completely differently.

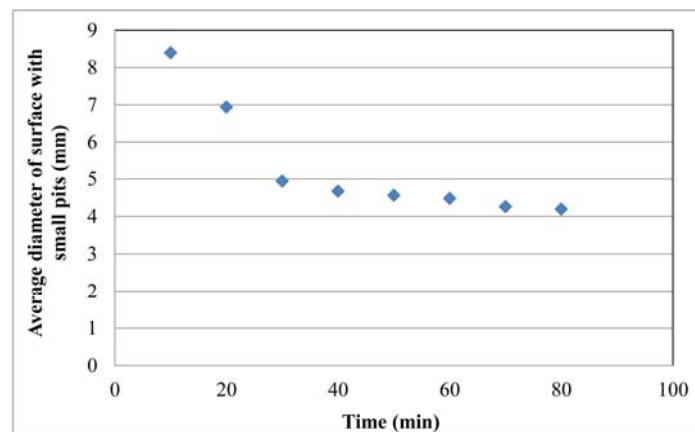


Fig.7. Average diameter of degradation surface area with small pits (inner circle diameter).

Formation of erosion ring was observed after 5 minutes of testing, since the ring border appeared with diameter close to the diameter of used horn. After 80 minutes of testing, the ring is almost completely formed, but there are still small areas with less or no degradation. In the initial period of erosion ring formation, larger pits are observed at the zone between outer and inner edge of ring, in the region around the horn perimeter. Small pits are detected in the central area of degraded or exposed surface that is also center of the ring. Area of larger pits (zone between inner and outer ring) was increasing at the expense of inner ring area with small pits (area inside the inner diameter) with increasing the cavitation exposure time. Hence, degradation area with larger pits occurred at the outer limits and propagates toward the center of the ring.

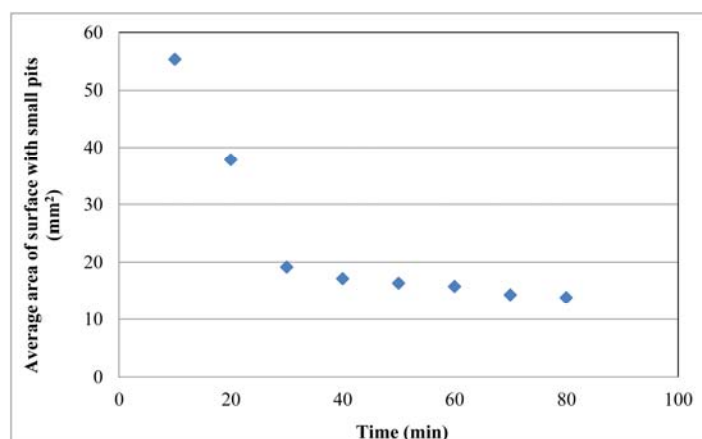


Fig. 8. Average degradation area of surface with small pits (area of inner circle).

3.5 Thermal imaging

The same conditions (heating for 90 seconds, photographs after 480 seconds of cooling) as in previous experiment related to the cordierite samples were applied [24]. Figure 9 shows results of thermal vision analysis of the samples based on zircon.

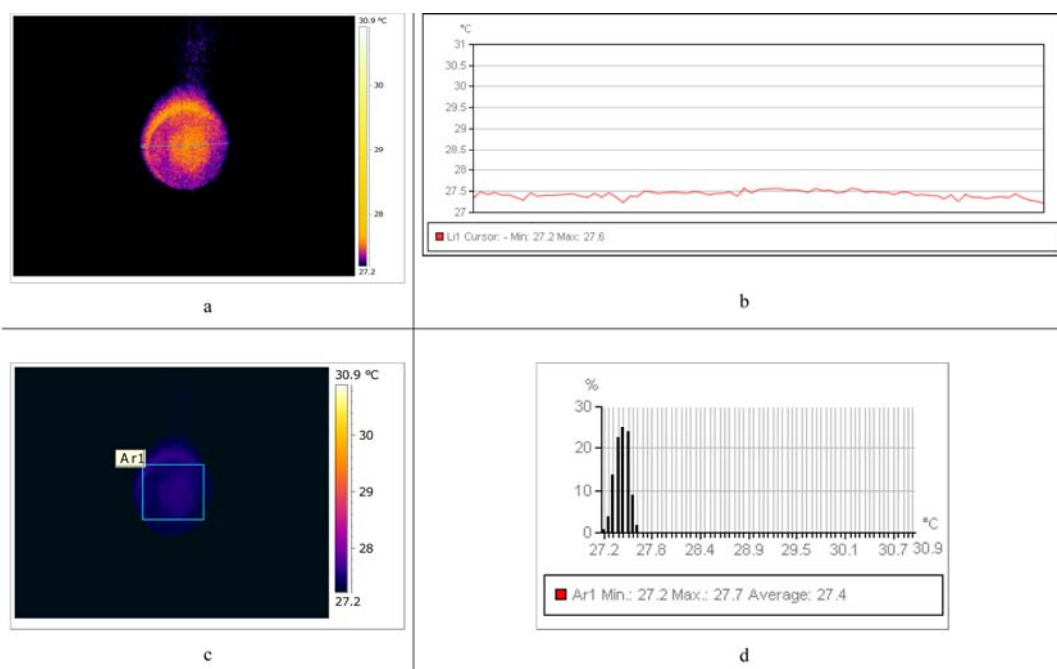


Fig. 9. Thermal imaging of zircon samples sintered at 1200 °C: a,c) sample thermographic images; b) temperature line profile and d) histogram of temperature distribution.

The thermograms given in Fig. 9 (a,c) show differences in damaged and undamaged zones, which correlate with the photographs in Fig. 4. Damaged and undamaged zones cannot be identified precisely based on the temperature line profiles shown in Fig. 9b). Based on these results, only distribution of the defects can be determined. The temperature distribution histograms, presented in Fig. 9d), indicate more regular temperature distribution of the zircon samples sintered at 1200 °C, and it also shows that pits depths of zircon samples sintered at

1200 °C in deformation zone correlates with the results obtained by image analysis.

4. Conclusion

Monitoring the damage level on the surface of the sintered zircon samples at 1200 °C several approaches were used: changes of mass loss, measuring of surface degradation by determining area of surface degradation, line profiles, and ring formation analysis using image analysis as well as thermal imaging analysis for obtaining the temperature profile and temperature distribution histogram. Results showed that the cavitation erosion of sintered zircon sample is characterized by occurrence of small pits, and that their number grows during the test. Results of measuring the surface level degradation reliably demonstrated the high quality of zircon samples exposed to cavitation erosion. Chosen methods of image and thermal analysis fully contributes to the characterization of zircon sample in terms of cavitation erosion and can be used for rapid and reliable selection of materials for use in this conditions.

Acknowledgments

This research has been financed by Ministry of Education, Science and Technological Development of the Republic of Serbia as part of the projects TR 33007, III 45012, TR 35002 and OI 172060.

5. References

1. P. Patnaik, Handbook of inorganic chemicals, McGraw-Hill Companies, New York, 2003.
2. D. R. Lide, Handbook of chemistry and physics, eighty seventh ed., CRC Press, Boca Raton, 1998.
3. R. E. Moore, Refractories, structure and properties, Encyclopedia of Materials: Science and Technology, Pergamon Press, Oxford, 2001.
4. F. L. Pirkle, D. A. Podmeyer, Zircon: origin and uses, Transactions, vol. 292, Society for Mining, Metallurgy and Exploration, Inc., USA 1988.
5. M. Senthil Kumar, A. Elayapermual, G. Senguttuvan, J. Ovonic Res., 7(5) (2011) 99.
6. R. Oberacker, Powder compaction by dry pressing, in: R. Riedel, I-Wei Chen (Eds.), Ceramics Science and Technology, Part 1-Synthesis and Processing, Vol. 3, first ed., Wiley-VCH Verlag GmbH&Co.KGaA (2012) 1.
7. Z. Pedzicha, R. Jasionowski, M. Ziabka, J. Eur. Ceram. Soc., 34 (2014) 3351.
8. S. Martinovic, M. Dojcinovic, M. Dimitrijevic, A. Devecerski, B. Matovic, T. Volkov Husovic, J. Eur. Ceram. Soc., 30 (2010) 3303.
9. S. Martinovic, M. Vlahovic, M. Dojcinovic, T. Volkov-Husovic, J. Majstorovic, Int. J. Appl. Ceram. Tec., 8(5) (2011) 1115.
10. F. G. Hammit, Cavitation and multiphase flow phenomena, McGraw-Hill, New York, 1980.
11. R. T. Knapp, J. W. Daily, F. G. Hammit, Cavitation, McGraw-Hill, New York, 1970.
12. T. Okada, Y. Iwai, S. Hattori, N. Tanimura, Wear, 184 (1995) 231.
13. S. Hattori, H. Mori, T. Okada, J. Fluid. Eng.-T ASME, 1201 (1998) 179.
14. Test method for cavitation erosion using vibratory apparatus, ASTM Standard G32-92, Annual Book of ASTM Standards, Vol. 03.02, ASTM, Philadelphia, 1992.

15. ASRM Standard G32-98 Standard, Test method for cavitation erosion using vibratory apparatus, Annual Book of ASTM Standards, pp. 107–120, 2000.
16. M. Dojcinovic, T. Volkov-Husovic, Mater.Lett., 62 (2008) 953.
17. G. Bregliozzi, A. Di Schino, SI.-U.Ahmed, J.M. Kenny, H. Haefke, Wear, 258 (2005) 503.
18. W. J. Tomlinson, A. S. Bransden, Wear, 185 (1995) 59.
19. C. J. Lin, J. L. He, Wear, 259 (2005) 154.
20. A. Krella, A. Czyzniewski, Wear, 260 (2006) 1324.
21. F. T. Cheng, C. T. Kwok, H. C. Man, Surf.Coat.Tech., 139 (2001) 14.
22. C. Feng, J. Shuyun, Appl. Surf.Sci., 292 (2014) 16.
23. N. Qiu, L. Wang, S. Wu, D.S. Likhachev, Eng. Fail. Anal., 55 (2015) 208.
24. M. Pavlovic, M. Dojcinovic, S. Martinovic, M. Vlahovic, Z. Stevic, T.Volkov-Husovic, Compos. Part B- Eng., 97 (2016) 84.
25. S. Martinovic, M. Vlahovic, M. Boljanac, M. Dojcinovic, T.Volkov-Husovic, J. Eur. Ceram.Soc., 33(1) (2013) 7.
26. G. Garcia-Atance Fatjó, M. Hadfield, K. Tabeshfar, Ceram. Int., 37 (2011) 1919.
27. Image Pro Plus, The Proven Solution for Image Analysis, Media Cybernetics, 1993.
28. X. P. V. Maldague, Theory and practice of infrared thermography for nondestructive testing, Wiley, New York, 2001.
29. C. Meola, Mater. Lett., 6(3) (2007) 747.
30. S. Sfarra, C. Ibarra-Castanedo, C. Santulli, F. Sarasini, D. Ambrosini, D. Paoletti, X. P. V. Maldague, Strain, 49(2) (2013) 175.
31. M. M. Dimitrijevic, M. Dojčinović, A. Devecerski, R. Jančić Heinemann, T. Volkov-Husovic, Sci. of Sinter., 45(1) (2013) 97.
32. A. Crinière, J. Dumoulin, C. Ibarra-Castanedo, X. Maldague, Quant. Infrared.Thermogr. J., 111 (2014) 84.
33. Y. Duan, S. Huebner, U. Hassler, A. Osman, C. Ibarra-Castanedo, X. P. V. Maldague, Infrared. Phys.Technol., 60 (2013) 275.
34. P. Theodorakeas, C. Ibarra-Castanedo, S. Sfarra, N. P. Avdelidis, M. Kouli, X. P. V. Maldague, D. Paoletti, D. Ambrosini, NDT. E. Int., 47 (2012) 150.
35. S. Sfarra, C. Ibarra-Castanedo, S. Ridolfi, G. Cerichelli, D. Ambrosini, D. Paoletti, X. Maldague, Appl. Phys. A. Mater. Sci. Process., 115(3) (2014) 1041.
36. M. M. Dimitrijevic, M. Dojčinović, D. Trifunović, T. Volkov-Husovic, R. Jančić Heinemann, Sci. of Sinter., 48 (2016) 371.
37. M. Posarac-Markovic, Dj.Veljovic, A. Devecerski, B. Matovic, T. Volkov Husovic, Mater. Design., 52 (2013) 295.
38. Lj. Kljajevic, S. Nenadovic, M. Nenadovic, D. Gautam, T. Volkov Husovic, A. Devecerski, B. Matovic, Ceram. Int., 39(5) (2013) 5467.

Садржај: У овом истраживању испитиван је механички удар индукован кавитационом ерозијом на керамички материјал на бази циркона. Са циљем одређивања нивоа деградације материјала, праћена је промена неколико параметара током испитивања кавитационе ерозије. Праћен је губитак масе као конвенционални критеријум за деградацију материјала, док је ниво деградације површине праћен анализом слике и термалном анализом. Резултати су показали висок степен кавитационе отпорности керамике на бази циркона, као и то да су овакви материјали погодни за примену у условима када се очекује озбиљна кавитациона ерозија.

Кључне речи: кермика на бази циркона; кавитациона ерозија; губитак масе; анализа слике; термална анализа.

© 2016 Authors. Published by the International Institute for the Science of Sintering. This article is an open access article distributed under the terms and conditions of the Creative Commons — Attribution 4.0 International license (<https://creativecommons.org/licenses/by/4.0/>).

